Chapter 4
FEC Scheme I in the DLC Protocol of Wireless ATM

In this chapter, a PCC scheme with two-level flexible UEP is constructed to apply to the header and various payloads of wireless ATM cell. Since their perforation matrices are programmable, the code rates of PCCs are applicable to the different sensitivity of source encoded symbols, even if only the same encoding and decoding hardwares are used. Their performance on Gaussian, Rayleigh and Ricean fading channels are deeply analyzed, and the PCC schemes make significant reductions in CLR and good balances for CLR and payload BER. This chapter contains a detailed study of the effect of code and channel parameters, and the contrasting performance of hard and soft decisions on the received symbols. The study clearly highlights the need for soft decisions and channel state information (CSI) to extract the maximum benefit from Viterbi decoding on fading channel.

4.1 Fundamentals of RCPC Codes

After adding a rate-compatibility restriction to the puncturing rule, PCCs can be extended to generate a family of RCPC codes [39]. The rate-compatibility restriction implies that all the code bits of a high rate PCC are used by lower rate CCs of the family.

RCPC codes are able to implement a multirate CC encoder/decoder simply. In Figure 4.1, the ordered information bits are shifted into a shift register of q-rate code. During the n_1 information bits, the R_1 code with the perforation matrix a_1 is used for multiplexing. As soon as the first bit of the second group enters the encoder, the perforation matrix a_2 will be used. After another n_3 information bits or the encoder shifts, the matrix is switched to a_3. At the p-th step, n_p/R_p code bits are transmitted per n_p information bits with the perforation matrix a_p and rate R_p . The frame is terminated after the group n_q by shifting $(K-1)$'s "0" bits into the shift register, where K is the constraint length of the original code. Thus, transmitting $(K-1)/R_q$ overhead code bits is necessary for the proper termination of the trellis.

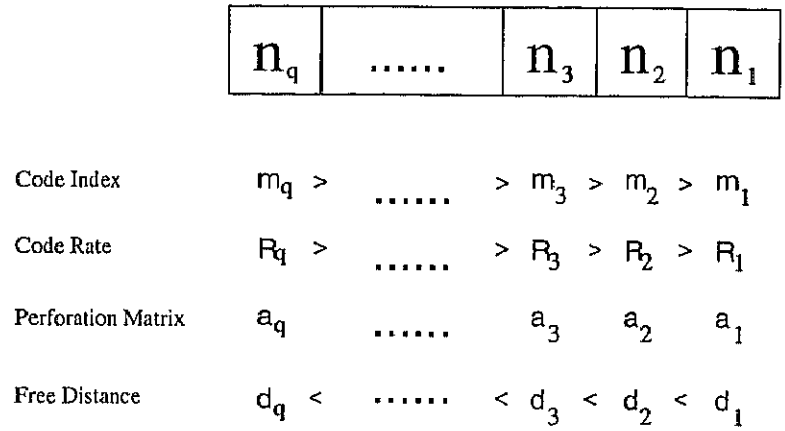

Figure 4.1: **Data frame with information bits grouped according to their SSI**

The procedure is easy to follow when n_p is an integer multiple of the puncturing period l. Then, the overall code rate is:

$$R = \frac{\sum_{p=1}^{q} n_p}{\sum_{p=1}^{q} \frac{n_p}{R_p} + \frac{K-1}{R_q}}. \tag{4.1}$$

When the original code is a $R = \frac{1}{3}$ CC and $l = 8$, a set of RCPC codes with UEP capabilities can be derived, whose rates are $R_p = \frac{l}{3l-m_p} = \frac{8}{24-m_p}$. The results of RCPC codes with $K = 4, 5, 6, 7$, $R_p = \frac{8}{24-m_p}$, where $m_p = 0, 1, \cdots, 15$, are obtained at [39]. In such a way, a whole family of codes with different rates is available using the same encoder and the same Viterbi decoder except for only the puncturing rule being changed. From these results, new FEC schemes for wireless ATM are constructed in the next section.

4.2 Two Coding Rate FEC Scheme Using RCPC Codes

The realization of two coding rate FEC scheme in the wireless interface of ATM is shown in Figure 4.2. Only the transmission from RM to BS is illustrated for simplicity. As in this figure, a wireless data packet header is added, the HEC is replaced by FEC-H and FEC-P in RM. In BS, after the validation by the decoder for the FEC-H and FEC-P, new HEC is inserted so as to become a normal ATM cell. There is a same procedure in the transmission from BS to RM. In our analysis, the wire-line portion of this system is assumed to be error free so that the encoding and decoding model of two rate RCPC codes is simplified, as shown in Figure 4.3. Let the coding rates of FEC-H and FEC-P be R_H and R_P ($R_H < R_P$), respectively. Obviously, from the

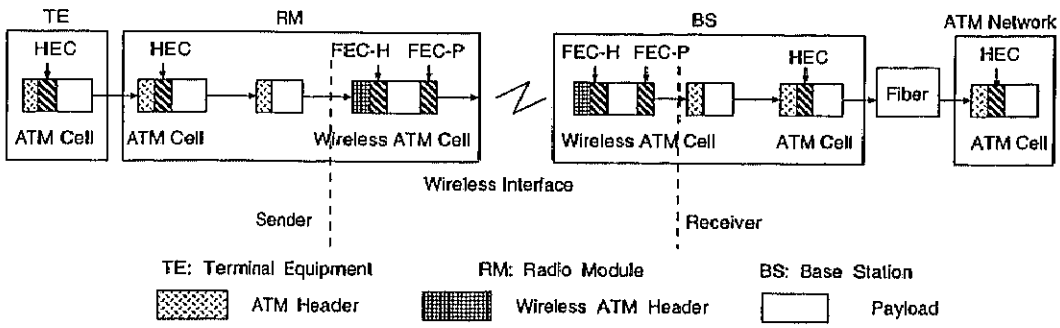

Figure 4.2: The realization of two rate FEC scheme in wireless ATM network

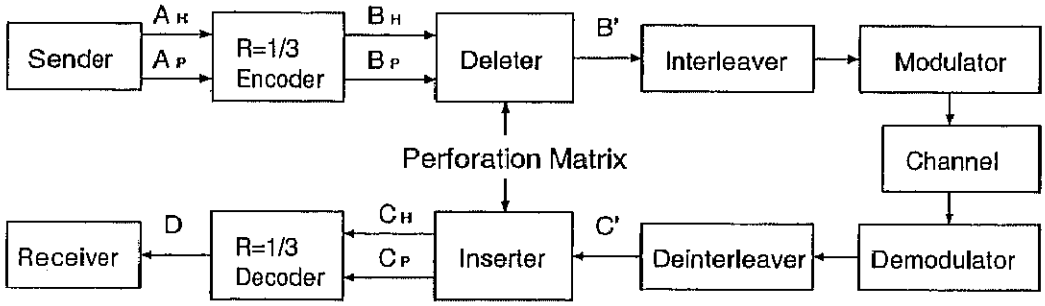

Figure 4.3: The encoding and decoding of two rates RCPC codes

selection of R_H and R_P, various overall rate R values of wireless ATM cell can be obtained. Supposing FEC-H be $R_H = \frac{8}{12}$ PCC and FEC-P be $R_P = \frac{8}{10}$ PCC, we have:

Header sequence ($A_H^{(i)}$): the more important bits (MIB: SSI is bigger), using $R_H = \frac{8}{12}$ PCC from (3,1,7) original CC, where $l_H = 8, m_H = 12$ and $n_H = 32 = 4l_H$;

Payload sequence ($A_P^{(i)}$): the less important bits (LIB: SSI is smaller), using $R_P = \frac{8}{10}$ PCC from (3,1,7) original CC, where $l_P = 8, m_P = 14$ and $n_P = 384 = 48l_P$.

When K=7, the overall code rate is:

$R = \frac{32+384}{32\frac{12}{8}+384\frac{10}{8}+6\frac{10}{8}} = \frac{832}{1071} \doteq 0.776$.

Let a data sequence from a sender be:

$$A^{(1)}, A^{(2)}, \ldots, A^{(i)}, \ldots, \tag{4.2}$$

where $A^{(i)}$=($A_H^{(i)}$,$A_P^{(i)}$), and the encoded data sequence $B^{(i)} = (B_H^{(i)}, B_P^{(i)})$ by (3,1) CC encoding is:

$$B_H^{(i)} = (B_{H,1}^{(i)}, B_{H,2}^{(i)}, \cdots, B_{H,4}^{(i)}), \tag{4.3}$$

$$\begin{aligned} B_{H,j}^{(i)} &= (b_{H,j,1}^{(i)}, b_{H,j,2}^{(i)}, \cdots, b_{H,j,24}^{(i)}), \\ B_{P}^{(i)} &= (B_{P,1}^{(i)}, B_{P,2}^{(i)}, \cdots, B_{P,48}^{(i)}), \\ B_{P,j}^{(i)} &= (b_{P,j,1}^{(i)}, b_{P,j,2}^{(i)}, \cdots, b_{P,j,24}^{(i)}), \end{aligned} \tag{4.4}$$

Suppose a perforation matrix of FEC-H be :

$$\begin{bmatrix} 1 & 1 & 1 & 1 & 1 & 1 & 1 & 1 \\ 1 & 0 & 1 & 0 & 1 & 0 & 1 & 0 \\ 0 & 0 & 0 & 0 & 0 & 0 & 0 & 0 \end{bmatrix},$$

and a perforation matrix of FEC-P be :

$$\begin{bmatrix} 1 & 1 & 1 & 1 & 1 & 1 & 1 & 1 \\ 1 & 0 & 0 & 0 & 1 & 0 & 0 & 0 \\ 0 & 0 & 0 & 0 & 0 & 0 & 0 & 0 \end{bmatrix}.$$

After deleting, the output data sequence $B'^{(i)} = (B_H'^{(i)}, B_P'^{(i)})$ becomes:

$$\begin{aligned} B_H'^{(i)} &= (B_{H,1}'^{(i)}, B_{H,2}'^{(i)}, \cdots, B_{H,4}'^{(i)}), \\ B_{H,j}'^{(i)} &= (b_{H,j,1}^{(i)}, b_{H,j,2}^{(i)}, b_{H,j,4}^{(i)}, b_{H,j,7}^{(i)}, b_{H,j,8}^{(i)}, b_{H,j,10}^{(i)}, b_{H,j,13}^{(i)}, \\ &\quad b_{H,j,14}^{(i)}, b_{H,j,16}^{(i)}, b_{H,j,19}^{(i)}, b_{H,j,20}^{(i)}, b_{H,j,22}^{(i)}), \end{aligned} \tag{4.5}$$

where $j = 1, \cdots, 4$, and:

$$\begin{aligned} B_P'^{(i)} &= (B_{P,1}'^{(i)}, B_{P,2}'^{(i)}, \cdots, B_{P,48}'^{(i)}), \\ B_{P,j}'^{(i)} &= (b_{P,j,1}^{(i)}, b_{P,j,2}^{(i)}, b_{P,j,4}^{(i)}, b_{P,j,7}^{(i)}, b_{P,j,10}^{(i)}, b_{P,j,13}^{(i)}, b_{P,j,14}^{(i)}, b_{P,j,16}^{(i)}, b_{P,j,19}^{(i)}, b_{P,j,22}^{(i)}), \end{aligned} \tag{4.6}$$

where $j = 1, \cdots, 48$.

After the transmission of $B'^{(i)}$ via channel, the de-interleaver outputs $C'^{(i)} = (C_H'^{(i)}, C_P'^{(i)})$ are:

$$\begin{aligned} C_H'^{(i)} &= (C_{H,1}'^{(i)}, C_{H,2}'^{(i)}, \cdots, C_{H,4}'^{(i)}), \\ C_{H,j}'^{(i)} &= (c_{H,j,1}^{(i)}, c_{H,j,2}^{(i)}, c_{H,j,4}^{(i)}, c_{H,j,7}^{(i)}, c_{H,j,8}^{(i)}, c_{H,j,10}^{(i)}, c_{H,j,13}^{(i)}, \\ &\quad c_{H,j,14}^{(i)}, c_{H,j,16}^{(i)}, c_{H,j,19}^{(i)}, c_{H,j,20}^{(i)}, c_{H,j,22}^{(i)}), \end{aligned} \tag{4.7}$$

where $j = 1, \cdots, 4$, and:

$$\begin{aligned} C_P'^{(i)} &= (C_{P,1}'^{(i)}, C_{P,2}'^{(i)}, \cdots, C_{P,48}'^{(i)}), \\ C_{P,j}'^{(i)} &= (c_{P,j,1}^{(i)}, c_{P,j,2}^{(i)}, c_{P,j,4}^{(i)}, c_{P,j,7}^{(i)}, c_{P,j,10}^{(i)}, c_{P,j,13}^{(i)}, c_{P,j,14}^{(i)}, c_{P,j,16}^{(i)}, c_{P,j,19}^{(i)}, c_{P,j,22}^{(i)}), \end{aligned} \tag{4.8}$$

where $j = 1, \cdots, 48$.

Then, by the inserter, we have $C^{(i)} = (C_H^{(i)}, C_P^{(i)})$:

$$\begin{aligned} C_H^{(i)} &= (C_{H,1}^{(i)}, C_{H,2}^{(i)}, \cdots, C_{H,4}^{(i)}), \\ C_{H,j}^{(i)} &= (c_{H,j,1}^{(i)}, c_{H,j,2}^{(i)}, \times, c_{H,j,4}^{(i)}, \times, \times, c_{H,j,7}^{(i)}, c_{H,j,8}^{(i)}, \\ &\quad \times, c_{H,j,10}^{(i)}, \times, \times, c_{H,j,13}^{(i)}, c_{H,j,14}^{(i)}, \times, c_{H,j,16}^{(i)}, \\ &\quad \times, \times, c_{H,j,19}^{(i)}, c_{H,j,20}^{(i)}, \times, c_{H,j,22}^{(i)}, \times, \times), \end{aligned} \tag{4.9}$$

where $j = 1, \cdots, 4$ and $\times$ represents an inserted dummy bit, and:

$$\begin{aligned} C_P^{(i)} &= (C_{P,1}^{(i)}, C_{P,2}^{(i)}, \cdots, C_{P,48}^{(i)}), \\ C_{P,j}^{(i)} &= (c_{P,j,1}^{(i)}, c_{P,j,2}^{(i)}, \times, c_{P,j,4}^{(i)}, \times, \times, c_{P,j,7}^{(i)}, \times, \\ &\quad \times, c_{P,j,10}^{(i)}, \times, \times, c_{P,j,13}^{(i)}, c_{P,j,14}^{(i)}, \times, c_{P,j,16}^{(i)}, \\ &\quad \times, \times, c_{P,j,19}^{(i)}, \times, \times, c_{P,j,22}^{(i)}, \times, \times), \end{aligned} \tag{4.10}$$

where $j = 1, \cdots, 48$.

Afterwards, through a $R = \frac{1}{3}$ decoder with $K = 7$, decoded bit sequence D is sent to the receiver.

In the above course, it is assumed that the bit synchronization and cell synchronization have been achieved. The decoder first decodes the header, if it succeeds, and then the QoS information identified in the header is extracted and used to determine the code rate used to decode the payload.

Using variable rate PCCs can also make the encoding rate (R_P) be assigned to each service having a different need of error protection. For example, we can set $R_H = \frac{8}{16} = \frac{1}{2}$ and $R_P = \frac{8}{10}$ for Audio, $R_P = \frac{8}{12}$ for Video, $R_P = \frac{8}{14}$ for Data. Its advantage is that only one encoder circuit and one decoder circuit are needed for FEC-H and various FEC-P even if their code rates, and thus the levels of error protection are different, because their perforation matrices are programmable. But in this case, the encoded length of wireless ATM cell becomes variable.

4.3 Performance Analysis over Gaussian and Fading Channel

One of the most important performance parameters in ATM cell transport is CLR, which is defined by the ratio of total lost cells to total transmitted cells. Here, suppose that ARQ is not implemented at the DLC sublayer and the MAC sublayer is ignored.

For the stream mode CBR/VBR services, when one or more bit errors are detected but cannot be corrected in the header, the cell will be misdirected and regarded as a lost cell outcome[51]. When an ATM cell is sent over a wireless interface, there are three possible outcomes:

1. The cell is accepted by the intended terminal.

2. The cell is accepted by the wrong terminal.

3. The cell is not accepted by any terminal.

It is assumed that the probability of the second outcome is negligibly small. In addition, there is a negligibly small probability that a cell accepted by the intended mobile will contain incorrect embedded QoS information. As a result, a header is either decoded correctly or the cell is lost [8]. Therefore, when a header portion contains errors that can not be corrected, the cell will be regarded as a lost cell outcome.

If the $R = \frac{l}{nl-m}$ PCC with the minimum free Hamming distance d_f is applied to the header (4 bytes), the probability of cell loss for coded systems is given by:

$$P_{\text{coded}} = 1 - (1 - P_c)^{32}, \tag{4.11}$$

where P_c is the bit error probability of wireless ATM header after using PCC. With the Viterbi decoding, P_c is upper bounded by [4]:

$$P_c \leq \frac{1}{l} \sum_{d=d_f}^{\infty} c_d P_d, \tag{4.12}$$

where c_d is the total number of error bits produced by the incorrect paths, which depends on the code, and P_d is the probability that a wrong path at distance d is selected, which depends on channel properties.

There are many models based on the empirical and analytical studies of real channels. In the following, we will discuss performance analysis of the proposed method in the cases of Gaussian channel, Rayleigh fading channel and Rice fading channel.

4.3.1 Performance over Gaussian Channel

For binary phase shift keying (BPSK) signal over Gaussian channel with soft decision, P_d is expressed by [4]:

$$P_d = \frac{1}{2}\text{erfc}(\sqrt{dRE_b/N_0}), \tag{4.13}$$

where E_b/N_0 is the SNR per uncoded bit, and erfc() is a complementary error function.

In case of hard decision, P_d is given by [4]:

$$P_d = \begin{cases} \sum_{i=\frac{d+1}{2}}^{d} {}_dC_i (1-P_b)^{d-i} P_b^i, & \text{for } d \text{ is odd,} \\ P_{d-1}, & \text{for } d \text{ is even,} \end{cases} \tag{4.14}$$

where P_b is the bit error probability over Gaussian channel without decoding being concerned:

$$P_b = \frac{1}{2}\text{erfc}(\sqrt{RE_b/N_0}). \tag{4.15}$$

For an uncoded header (4 bytes), the probability of cell loss is:

$$P_{\text{uncoded}} = 1 - (1 - P_b)^{32}. \tag{4.16}$$

For the HEC, there are two operating modes, as shown in Figure 2.7. In the correction mode, a single-bit error can be corrected and cells with multiple-bit errors are discarded. Its probability is: $P_{cor.} = P_0$. P_0 is the probability of no error in one cell header, which is equal to $(1 - P_b)^{40}$. In the detection mode, all cells with detected errors in header are discarded, its probability is: $P_{det.} = 1 - P_0$. Besides, the probability of the single-bit error in one cell header is $P_1 = 40P_b(1 - P_b)^{39}$, and the probability of multiple-bit errors in one cell header is $P_2 = 1 - P_0 - P_1$. Then, the probability of cell loss is:

$$P_{\text{HEC}} = P_{det.}(P_1 + P_2) + P_{cor.}P_2 = (1 - P_0)(1 - P_0) + P_0(1 - P_0 - P_1). \tag{4.17}$$

If an (n, k) t-error correction BC is applied to a header, the probability of cell loss is given by:

$$P_t = \sum_{i=t+1}^{n} {}_nC_i(1 - P_b)^{n-i}P_b^i. \tag{4.18}$$

Figures 4.4 to 4.11 depict the CLR versus E_b/N_0 analytic upper bound over Gaussian channel. The solid lines represent the results of $R_H = \frac{8}{12}$, $\frac{8}{16}$, $\frac{8}{20}$ and $\frac{8}{24}$ PCCs decoded by soft and hard decisions (PC-UEP1-s/h to PC-UEP4-s/h), the constraint length K of their same original code is 7 and 5. The dashed lines represent the results of the uncoded one, HEC, AWA and three different BCs, respectively. AWA represents (56,32) 4-bit error correction code for the header and (208,192) 2-bit error correction code for the payload[9]. BC1, BC2 and BC3 represents (28,16) 2-bit, (40,16) 4-bit and (49,16) 6-bit error correction codes, respectively [8]. From these figures, we know the performance of the BCs and the HEC remain almost the same, which means the BCs can not decrease the CLRs efficiently over Gaussian channel. The PCCs with soft and hard decisions decrease more CLR than the others, however, the improvement of the latter is smaller than the former. For example, the (16,8) PCC using soft decision realizes about 5.6 dB gain over the uncoded scheme, 3.2 dB gain over the HEC scheme and the BC2 scheme, 2.1 dB gain over the AWA scheme and 2.2 dB gain over the case of PCC with hard decision at a CLR of 10^{-6}. Note that the cases of K=7 have lower CLR than the cases of K=5. Obviously, the PCC schemes realize each result in these figures by increase of 50%, 100%, 150% or 200% bandwidth for a header than the uncoded scheme, and the BC schemes realize each

result in these figures by increase of 75%, 150%, or 206% bandwidth for the header than the uncoded scheme. The bandwidth increases for the header using AWA and HEC schemes are 75% and 25% higher than the uncoded scheme, respectively.

4.3.2 Performance over Rayleigh Fading Channel

Rayleigh model represents a worst case model for the design engineer while offering analytical convenience, where the direct wave is obstructed and the mobile unit receives only reflected waves. Rayleigh model arises from the combination of many point scatter contributions at the receiver, each having only a small fraction of the received energy. In this case, the receiving level is assumed to correspond to the Rayleigh distribution, which is frequently used to model multipath fading with no direct line-of-sight (LoS) path. Under the assumption of fully-interleaved, the channel is memoryless and produces independent data errors. For the BPSK signal over Rayleigh fading channel with soft decisions and full CSI, P_d can be upper bounded by [39]:

$$P_d \leq \frac{1}{2}\left(\frac{1}{1+RE_b/N_0}\right)^d. \tag{4.19}$$

For an uncoded header (4 bytes), a header with HEC and a header with an (n,k) t-error correcting BCs, their probabilities of cell loss are given by equations (4.16) to (4.18). When the header is protected with PCCs using hard decisions and no CSI, the CLR can be inferred from equations (4.11), (4.12) and (4.14). Note that P_b is the bit error probability over Rayleigh fading channel, which is given by [4]:

$$P_b = \frac{1}{2}\left(1-\sqrt{\frac{RE_b/N_0}{1+RE_b/N_0}}\right). \tag{4.20}$$

Figures 4.12 to 4.19 depict the CLR versus E_b/N_0 analytic upper bound over Rayleigh fading channel. Each curve in these figures represents the same one as in Figures 4.4 to 4.11. From these figures, we know the reduction of CLR by each PCCs is greater than those by the other schemes, and more effective than those over Gaussian channel. Though the CLR of PC-UEP1-h is almost equal to the one of BC1, the ones of PC-UEP3-h and PC-UEP4-h are better than the ones of BC2 and BC3, respectively. It is worth mentioning that the performance improvement increases much more when hard decision is substituted by soft decision. For example, the (16,8) PCC using soft decisions realizes over 30 dB gain over the uncoded scheme, about 28 dB gain over the HEC scheme, 12 dB gain over the (40,16) BC2 and AWA schemes, and 8 dB gain over the case of hard decisions using the same PCC at a CLR of 10^{-6}. For each result in these figures, there are the same increases in bandwidth for a header as in the case of Gaussian channel, shown in Figures 4.4 to 4.11. Obviously, the PCC schemes using soft decisions have much better CLR performance than the BC schemes with

the same increase in the required bandwidth, and the cases of K=7 have lower CLR than the cases of K=5.

4.3.3 Performance over Ricean Fading Channel

SHF may be suitable for wireless ATM systems because multimedia services require high speed transmission capability as high as 10Mbps. SHF system has a LoS transmission path, and then the received signal consists of a direct wave and a number of reflected waves. The direct wave is a stationary nonfading signal with a constant amplitude. The reflected waves are independent random multipath signals. That is to say, its receiving level is assumed to correspond to the Ricean distribution. So it is necessary to compare the performance of the PCC schemes over Ricean channel with the ones over Gaussian and Rayleigh fading channels.

For the non-frequency-selective Ricean fading channel with a multiplicative distortion r, the probability density function (pdf) of r is:

$$P(r) = 2r(1 + C/M)\exp[-(r^2(1 + C/M) + C/M)] \times \mathrm{I}_0(2r\sqrt{C/M(1 + C/M)}), \quad (4.21)$$

where $E(r^2)$=1, C/M is the ratio of the direct to diffusely related signal energy, and $\mathrm{I}_0()$ is the zeroth-order modified Bessel function of the first kind. Therefore, the probability of bit error for a Rice fading channel is expressed by:

$$P_b = \frac{1}{2}\int_0^\infty \mathrm{erfc}(r\sqrt{RE_b/N_0})P(r)dr. \quad (4.22)$$

In case of hard decision and no CSI, the probability P_d that a wrong path at distance d is selected is given by equation (4.14), where P_b is the bit error probabilities of the Gaussian, Rayleigh or Ricean fading channel, respectively.

Let C/M be 7 dB, which is typical for mobile communications to cars in open area. The CLR versus E_b/N_0 analytic upper bounds decoding with hard decisions and no CSI are depicted in Figures 4.20 to 4.23. For $R_H = \frac{8}{12}$, $\frac{8}{16}$, $\frac{8}{20}$ and $\frac{8}{24}$ PCC schemes (PC-UEP1 to PC-UEP4), the constraint length K of their same original code is 7. The solid lines represent the results over Ricean fading channels, the dashed lines represent the results over Gaussian and Rayleigh fading channels, respectively. The figures show that the upper bound of the CLR over the Ricean fading channel is between those over Gaussian and Rayleigh fading channels as expected, because its propagation condition is better than the one over the Rayleigh fading channel but worse than the one over the Gaussian channel for communication. For example, the SNR over Ricean fading channel needs about 13 dB, while the SNR over the Rayleigh fading channel needs about 21 dB, the SNR over Gaussian channel needs about 9 dB in the case of hard decisions using the same (16,8) PCC at a CLR of 10^{-6}.

4.3.4 Performance of Balance Between CLR and Payload BER

It is extremely efficient from the viewpoints of coding gain and coding rate to create the same balanced design for CLR and payload BER as HEC for wired ATM [34]. Figures 4.24 to 4.27 show the relationships of the CLRs and payload BERs over the fully interleaved Rayleigh fading channel. The dashed lines represent the results of the uncoded one for a header and a payload, the HEC for a header and the uncoded one for a payload, and the AWA system, respectively. The solid lines represent PC-UEP11, PC-UEP12, PC-UEP21, PC-UEP22, PC-UEP31, PC-UEP32, PC-UEP41, PC-UEP42 in below, the constraint length K of their same original code is 7.

PC-UEP11: $R_H = \frac{8}{12}$ and $R_P = \frac{8}{9}$,
PC-UEP12: $R_H = \frac{8}{12}$ and $R_P = \frac{8}{10}$;
PC-UEP21: $R_H = \frac{8}{16}$ and $R_P = \frac{8}{10}$,
PC-UEP22: $R_H = \frac{8}{16}$ and $R_P = \frac{8}{12}$;
PC-UEP31: $R_H = \frac{8}{20}$ and $R_P = \frac{8}{12}$,
PC-UEP32: $R_H = \frac{8}{20}$ and $R_P = \frac{8}{16}$;
PC-UEP41: $R_H = \frac{8}{24}$ and $R_P = \frac{8}{16}$,
PC-UEP42: $R_H = \frac{8}{24}$ and $R_P = \frac{8}{20}$.

These figures show that PC-UEP12, PC-UEP22, PC-UEP32 and PC-UEP42 are closer to HEC than AWA, i.e., their applications to wireless ATM networks are expected more similar performance to the application of HEC to the standard ATM networks. Therefore, they have better balances than AWA. For PC-UEP11, PC-UEP21 PC-UEP31 and PC-UEP41, owing to their less payload error-correction abilities and the same header error-correction abilities, the balances are not as good as those of PC-UEP12, PC-UEP22, PC-UEP32 and PC-UEP42, respectively.

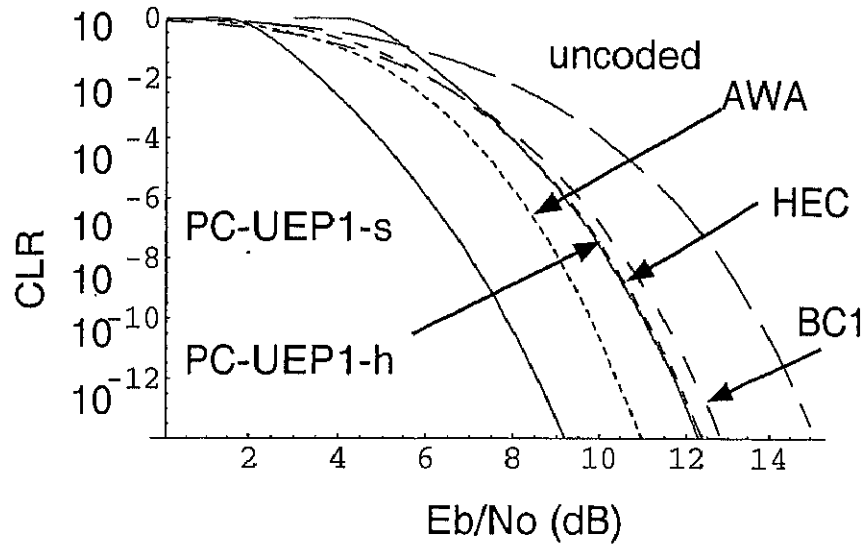

Figure 4.4: The CLR versus SNR analytic upper bound for PC-UEP1 over Gaussian channel (K=7)

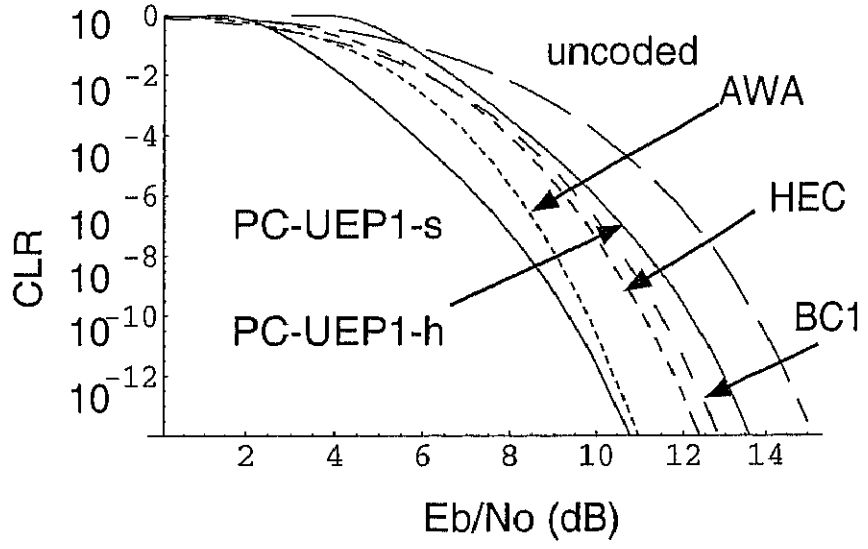

Figure 4.5: The CLR versus SNR analytic upper bound for PC-UEP1 over Gaussian channel (K=5)

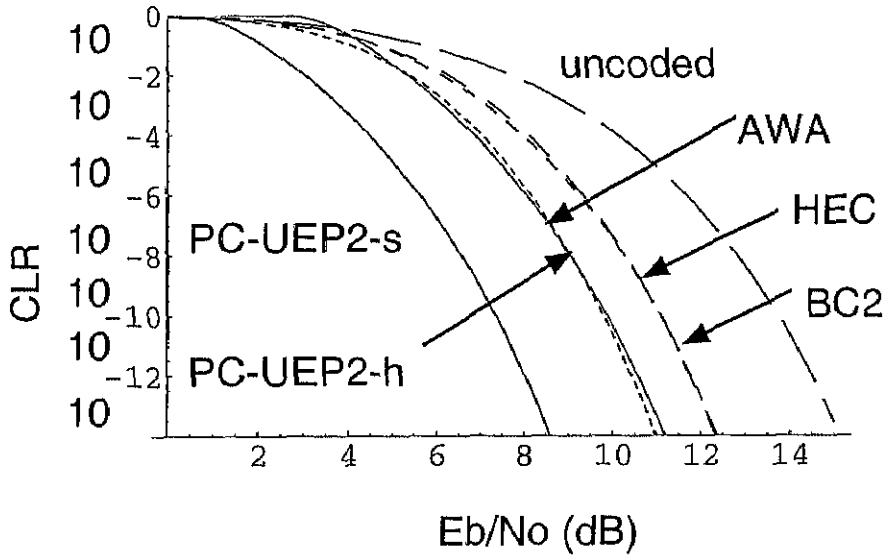

Figure 4.6: The CLR versus SNR analytic upper bound for PC-UEP2 over Gaussian channel (K=7)

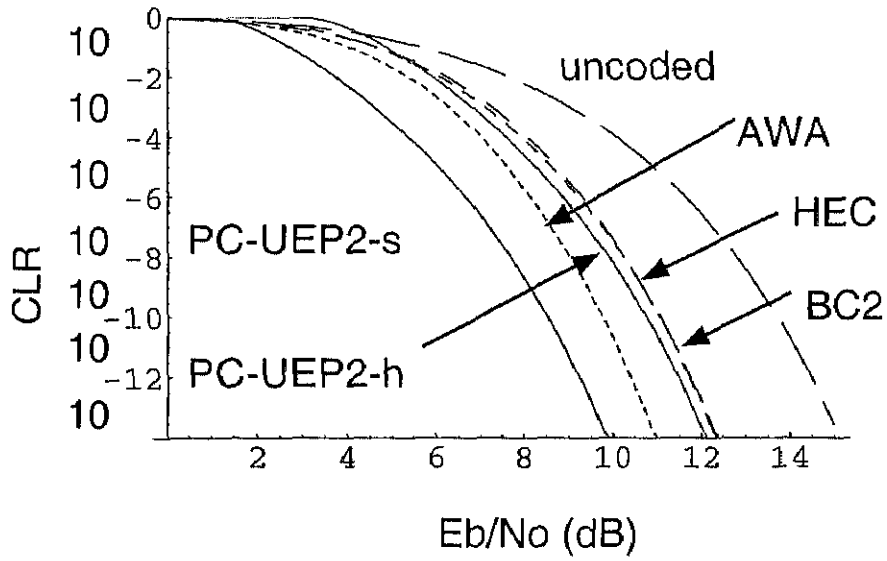

Figure 4.7: The CLR versus SNR analytic upper bound for PC-UEP2 over Gaussian channel (K=5)

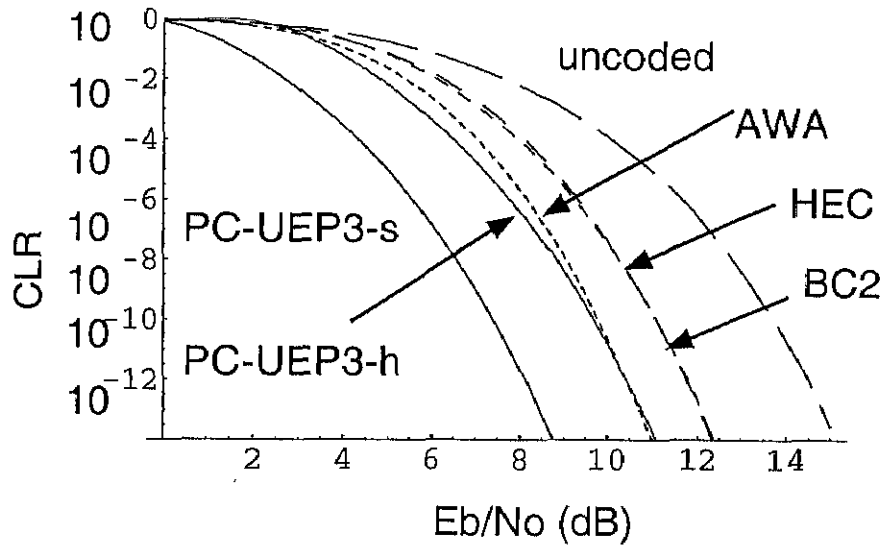

Figure 4.8: The CLR versus SNR analytic upper bound for PC-UEP3 over Gaussian channel (K=7)

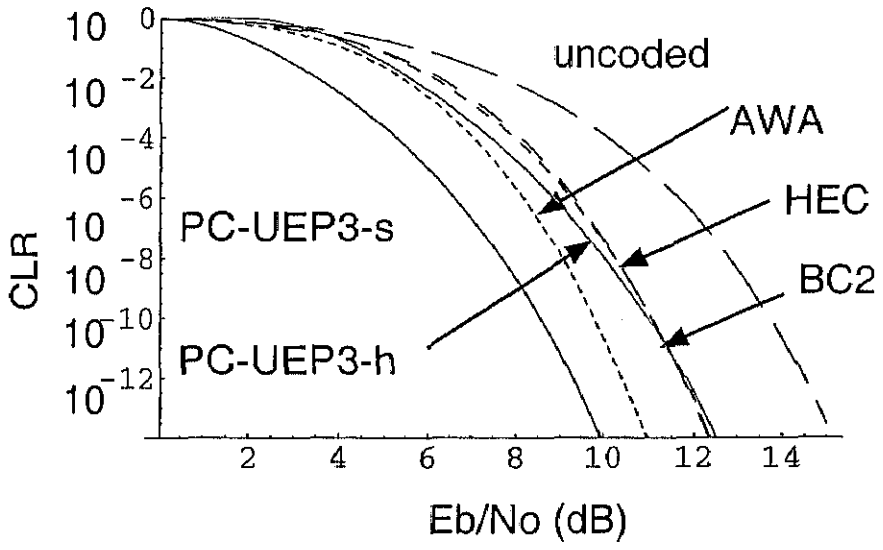

Figure 4.9: The CLR versus SNR analytic upper bound for PC-UEP3 over Gaussian channel (K=5)

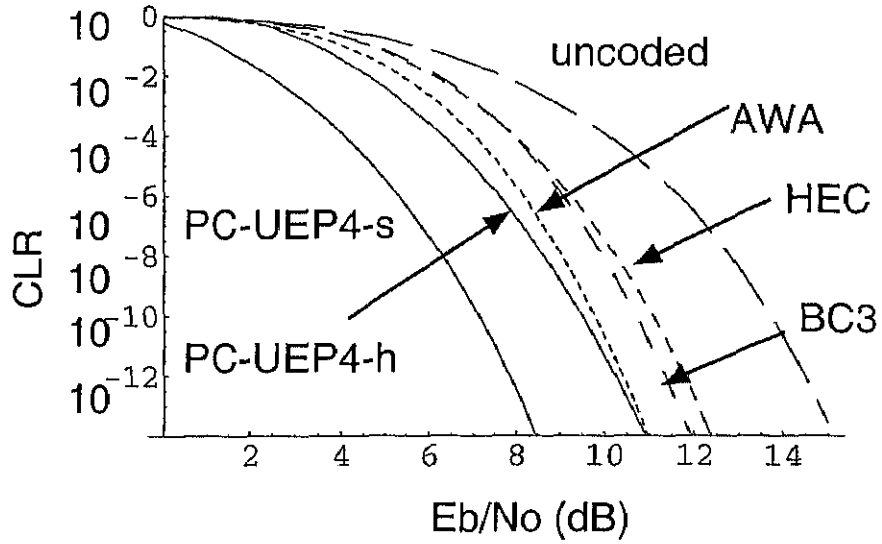

Figure 4.10: The CLR versus SNR analytic upper bound for PC-UEP4 over Gaussian channel (K=7)

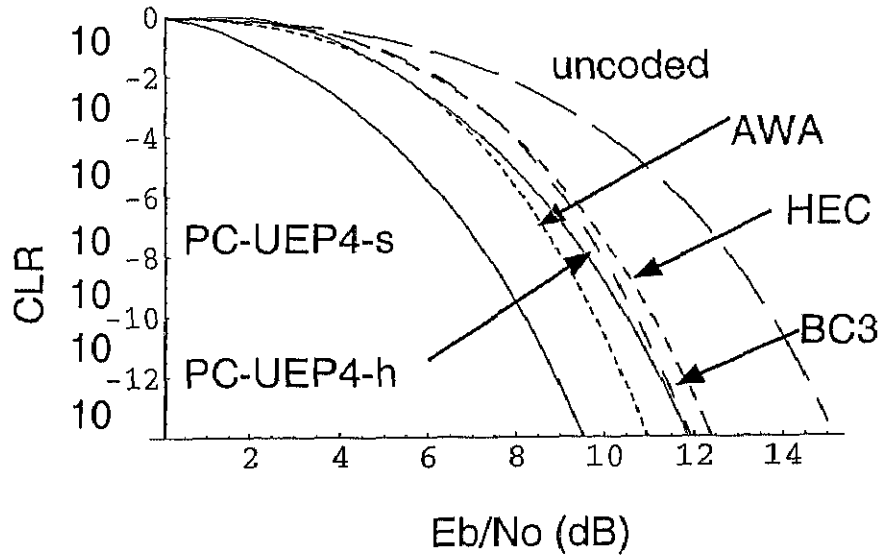

Figure 4.11: The CLR versus SNR analytic upper bound for PC-UEP4 over Gaussian channel (K=5)

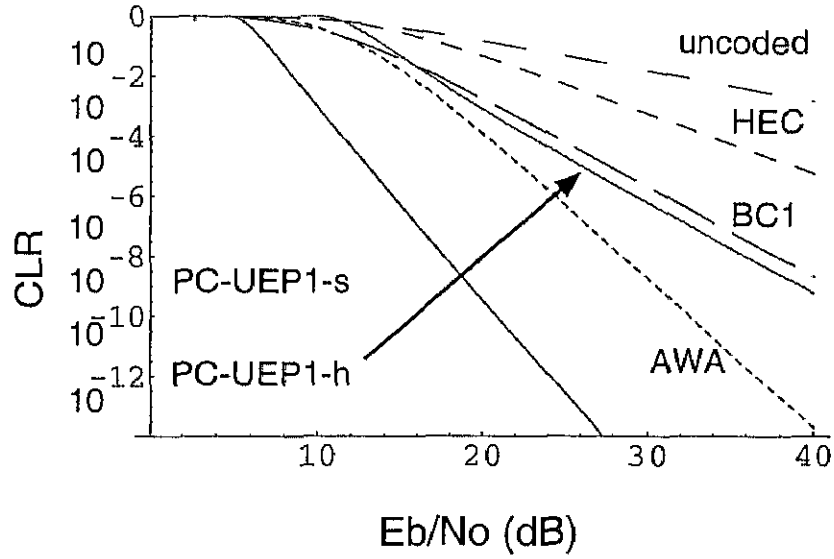

Figure 4.12: The CLR versus SNR analytic upper bound for PC-UEP1 over Rayleigh fading channel (K=7)

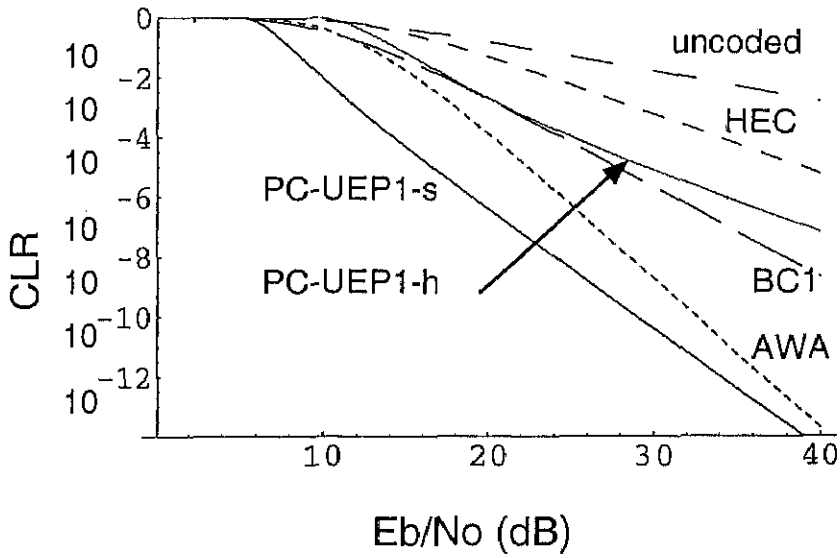

Figure 4.13: The CLR versus SNR analytic upper bound for PC-UEP1 over Rayleigh fading channel (K=5)

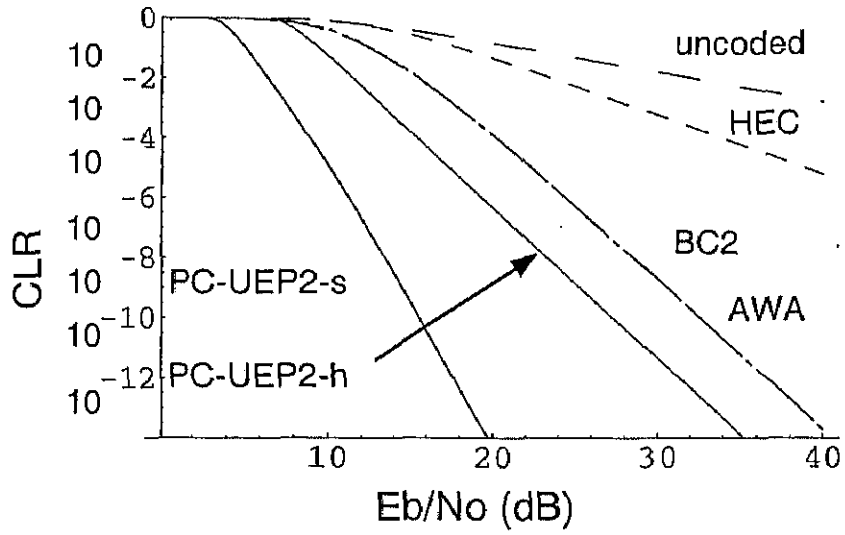

Figure 4.14: The CLR versus SNR analytic upper bound for PC-UEP2 over Rayleigh fading channel (K=7)

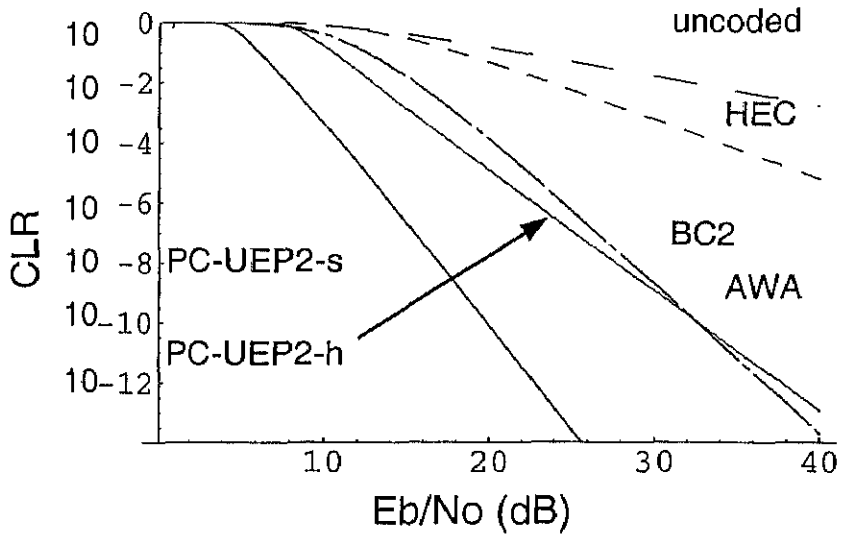

Figure 4.15: The CLR versus SNR analytic upper bound for PC-UEP2 over Rayleigh fading channel (K=5)

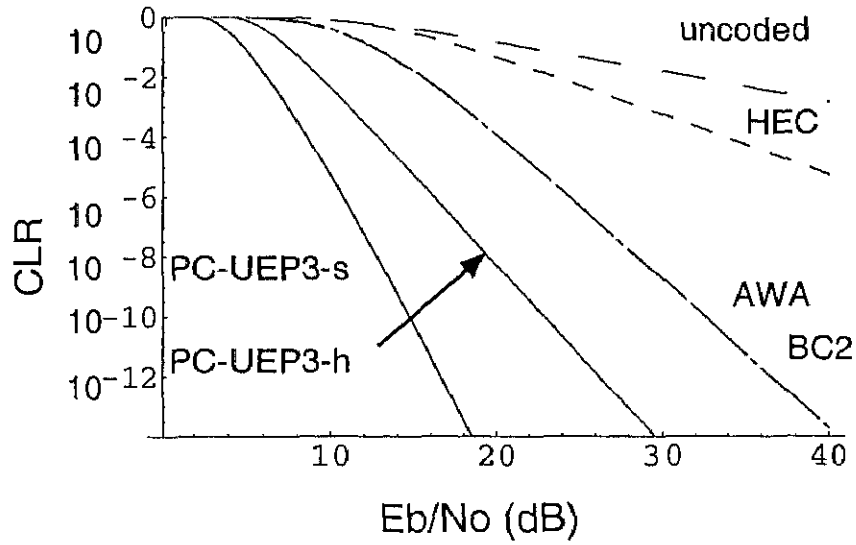

Figure 4.16: The CLR versus SNR analytic upper bound for PC-UEP3 over Rayleigh fading channel (K=7)

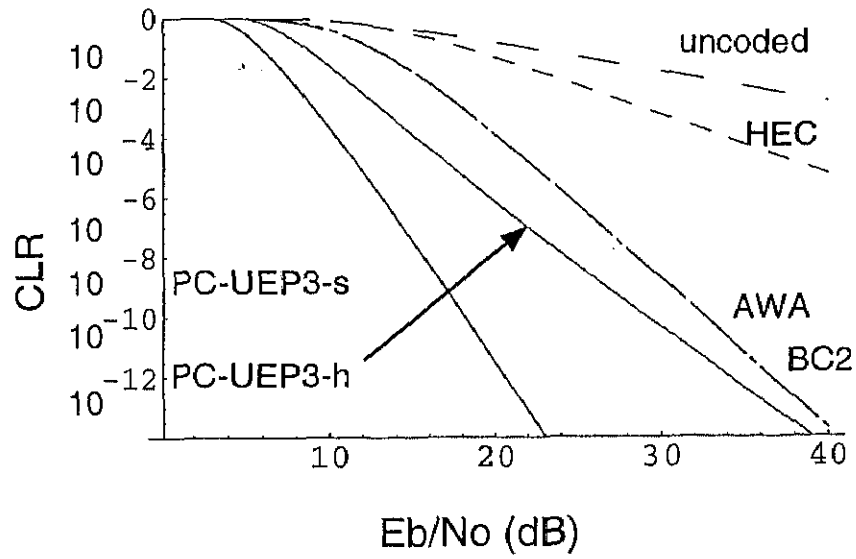

Figure 4.17: The CLR versus SNR analytic upper bound for PC-UEP3 over Rayleigh fading channel (K=5)

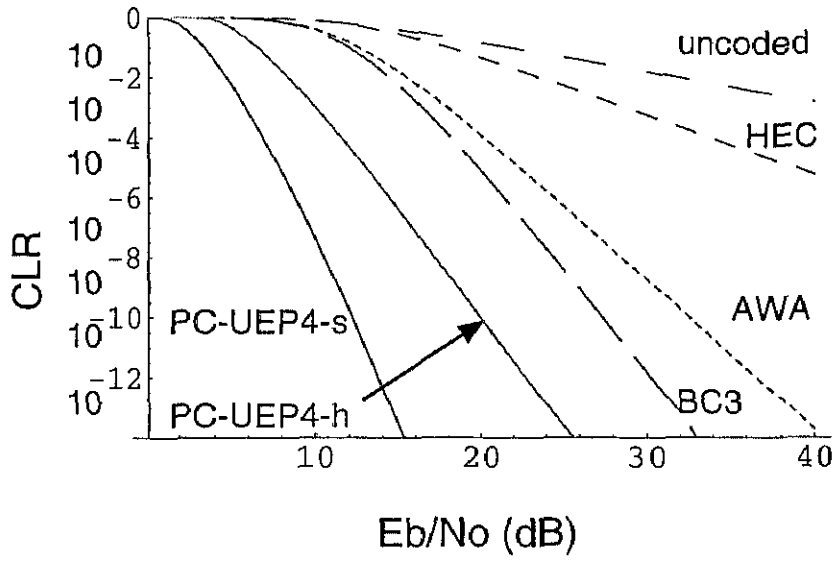

Figure 4.18: The CLR versus SNR analytic upper bound for PC-UEP4 over Rayleigh fading channel (K=7)

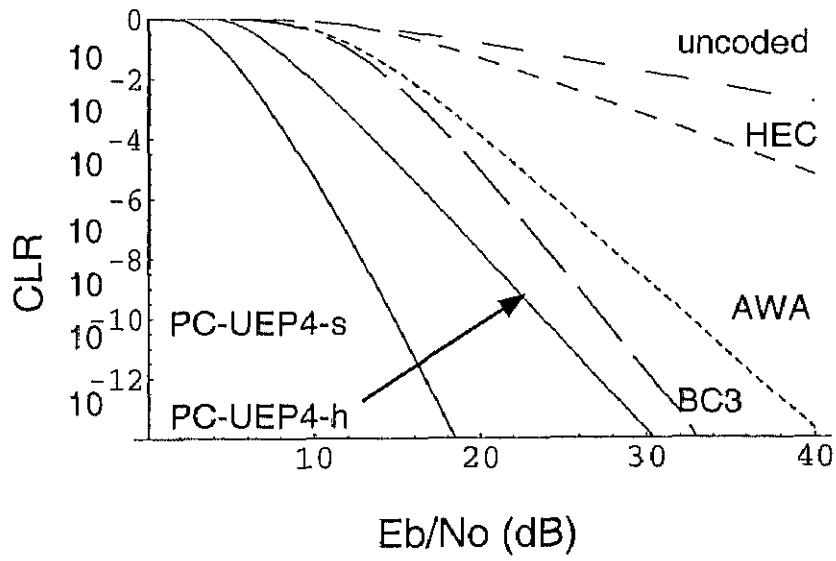

Figure 4.19: The CLR versus SNR analytic upper bound for PC-UEP4 over Rayleigh fading channel (K=5)

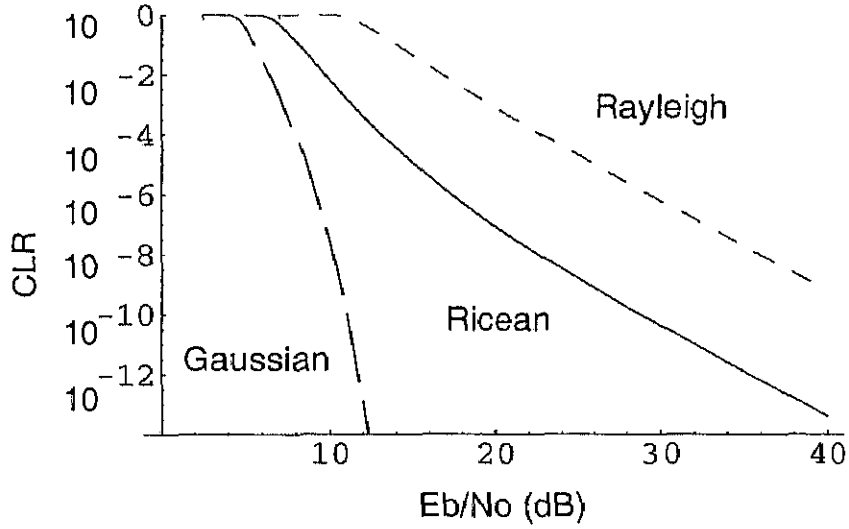

Figure 4.20: The CLR versus SNR analytic upper bound for PC-UEP1 over Gaussian and fading channel (K=7)

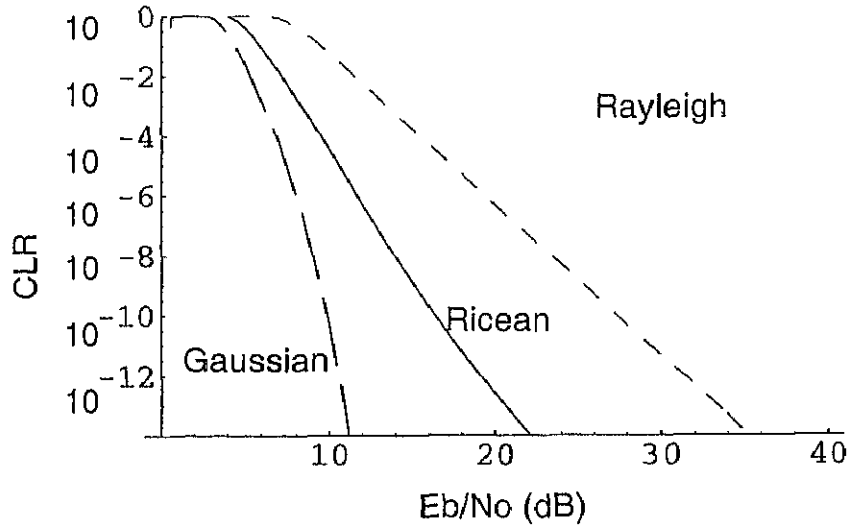

Figure 4.21: The CLR versus SNR analytic upper bound for PC-UEP2 over Gaussian and fading channel (K=7)

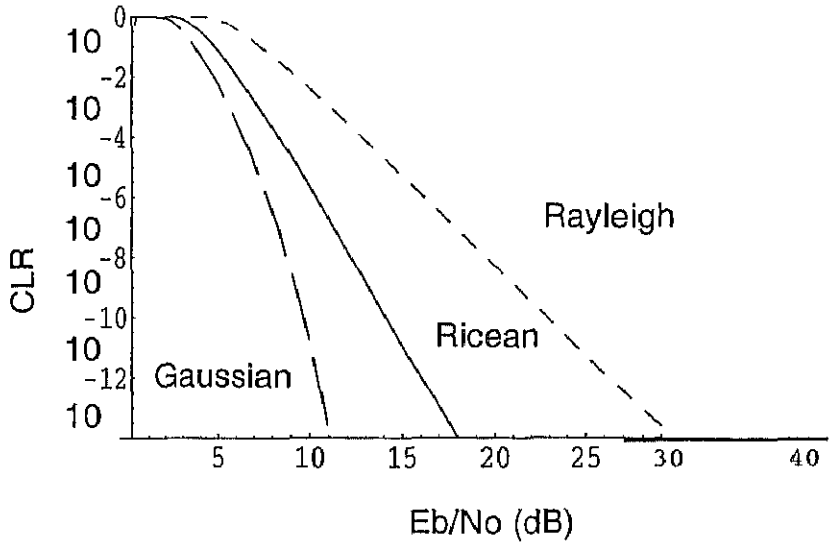

Figure 4.22: The CLR versus SNR analytic upper bound for PC-UEP3 over Gaussian and fading channel (K=7)

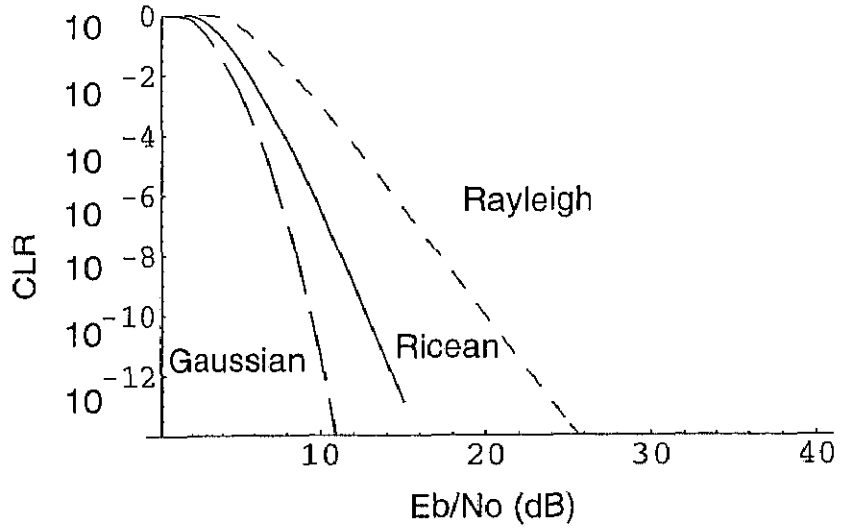

Figure 4.23: The CLR versus SNR analytic upper bound for PC-UEP4 over Gaussian and fading channel (K=7)

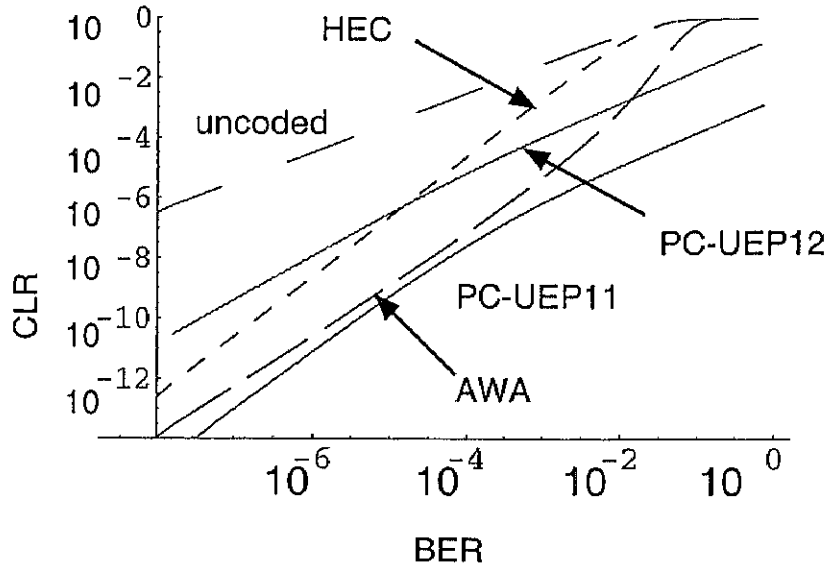

Figure 4.24: The CLR versus payload BER analytic upper bound for PC-UEP1 (K=7)

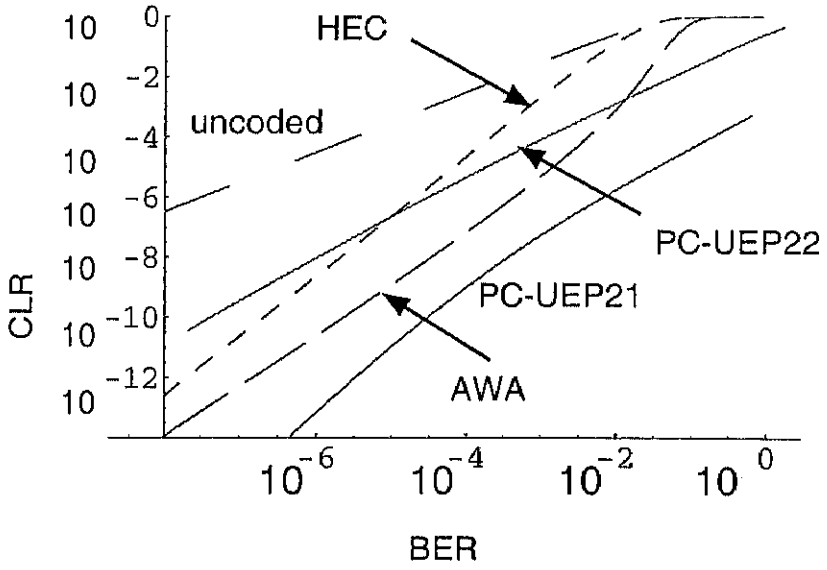

Figure 4.25: The CLR versus payload BER analytic upper bound for PC-UEP2 (K=7)

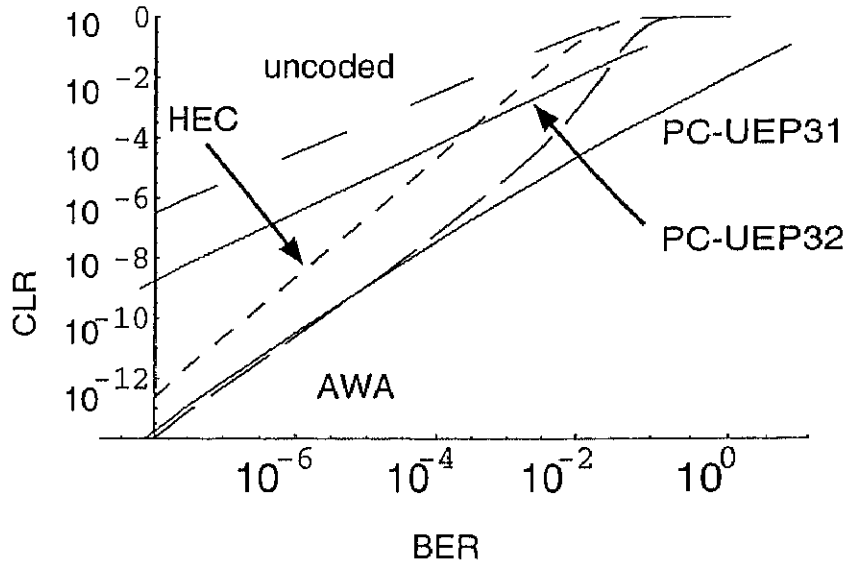

Figure 4.26: The CLR versus payload BER analytic upper bound for PC-UEP3 (K=7)

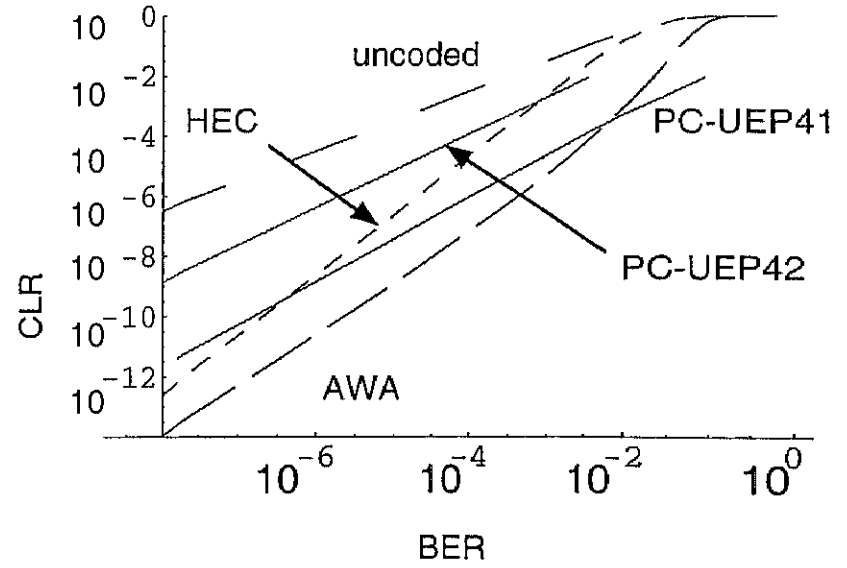

Figure 4.27: The CLR versus payload BER analytic upper bound for PC-UEP4 (K=7)